

Diameter-Dependent Bending Modulus of Individual Multiwall Boron Nitride Nanotubes

*Adrienne E. Tanur[†], Jiesheng Wang[‡], Arava L. M. Reddy[§], Daniel N. Lamont[§], Yoke Khin Yap[‡],
Gilbert C. Walker^{†§*}*

[†]Department of Chemistry, University of Toronto, Toronto, Ontario M5S 3H6, [‡]Department of Physics, Michigan Technological University, Houghton, Michigan 49931-1295, [§]Department of Chemistry, University of Pittsburgh, Pittsburgh, Pennsylvania 15260

[*walker@chem.utoronto.ca](mailto:walker@chem.utoronto.ca)

Supporting Information

Determination of Spring Constant.....	2
Error Analysis.....	4
Investigation of Inner and Outer Tube Diameter.....	4
Force Mapping Technique.....	5

Determination of Spring Constant

The spring constants of the AFM cantilevers used were determined by the thermal method described by Hutter and Bechhoefer.¹ The thermal method is reliable for measuring small (< 1 N/m) spring constant cantilevers (i.e. results in errors of ~ 5 -10%), because their relatively large thermal oscillation amplitude (< 1 Å). The method can have a larger error when applied to stiff (> 10 N/m) cantilevers because of their smaller thermal oscillation amplitudes (< 10 pm), which can result in a poor signal-to-noise ratio.² In order to demonstrate the applicability of the thermal method to the stiff cantilevers used in this work, we present the details of our spring constant determination method, which is based on the thermal method.

The first step in the process is the determination of the deflection (inverse) optical lever sensitivity, which is achieved by collecting force curves from a clean Si substrate and fitting the contact region. Next, a power spectral density plot is acquired via the thermal tune function within the AFM software (MFP-3D v090909, Asylum Research, CA; Igor Pro v6.12, Wavemetrics, OR). A typical PSD plot obtained from a Si probe (NCH, Nano World, Neuchâtel Switzerland) is shown in Figure 1 below.

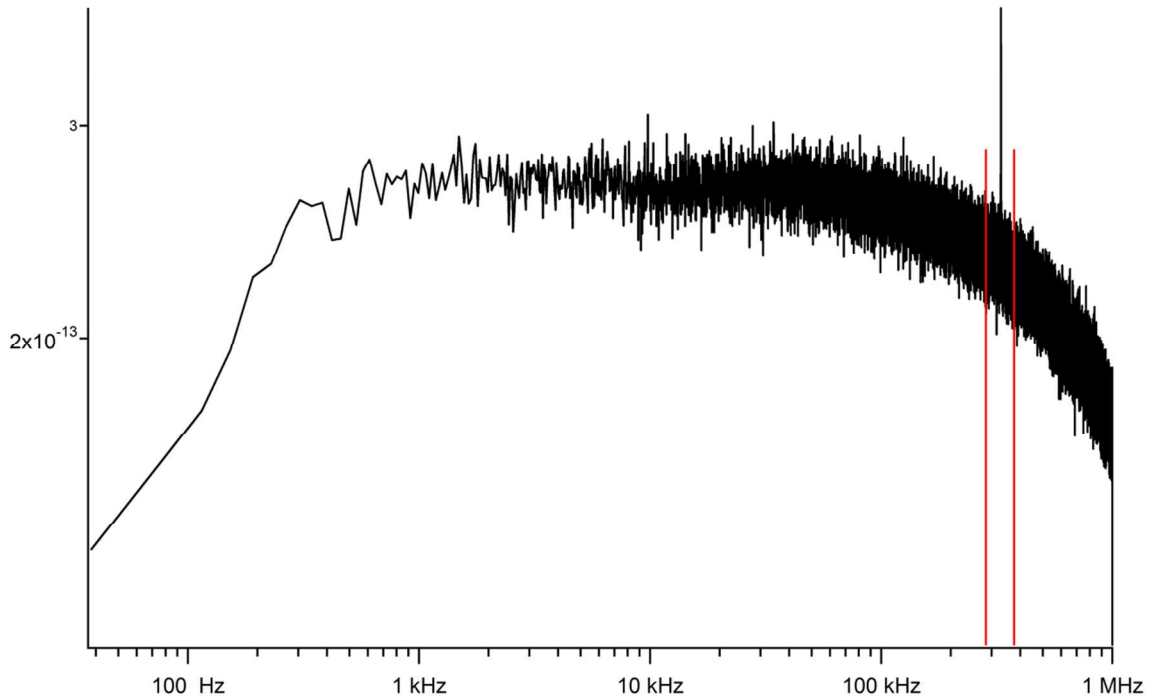


Figure 1: Power spectral density plot for Si cantilever

Figure 2 shows the details of the region containing the first resonance peak (the frequency range is indicated in red in Figure 1). The total PSD is shown in black and the thermal peak fit (damped harmonic oscillator model, Lorentzian lineshape) is shown in blue. The

quality factor of this peak is 460, and the signal-to-noise ratio is approximately 16 (intensity of peak:standard deviation of baseline). This signal-to-noise ratio is sufficient for the software to fit the resonance peak without difficulty, and based on the fit parameters the spring constant was calculated by the AFM software using the equations of Hutter and Bechhoefer.¹ The error is estimated to be less than 20%, with the error in the optical lever sensitivity being the major contributor.³ The spring constants of the cantilevers used in this study were found to range from 33 – 46 N/m. The manufacturer lists the nominal spring constant as 42 N/m, and indicates that a typical range is 21 – 78 N/m.⁴ Because the signal-to-noise ratio is high enough to obtain a good fit to the resonance peak, the estimated error of 20% associated with thermal method performed with our instrumentation and software is appropriate for the spring constant error.

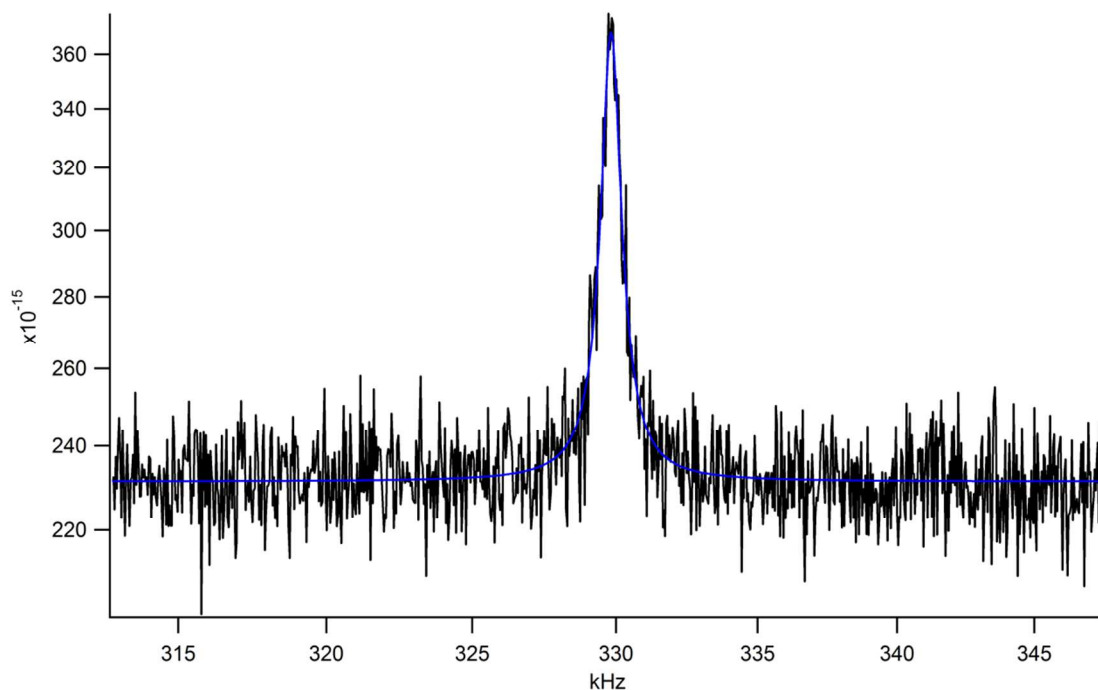


Figure 2: Region of PSD plot containing first resonance peak

References

1. Hutter, J. L.; Bechhoefer, J., Calibration of atomic-force microscope tips. *Rev Sci Instrum* 1993, 64, 1868-1873.
2. Ohler, B., Cantilever spring constant calibration using laser Doppler vibrometry. *Rev Sci Instrum* 2007, 78, 063701-5.
3. Fuierer, R., MFP-3D Procedural Operation 'Manualette' v10. Asylum Research: Santa Barbara, 2008.
4. NanoWorld Type NCH: Non-contact / Tapping™ mode - High resonance frequency. <http://www.nanoworld.com/pointprobe-tapping-mode-afm-tip-nch>.

Error Analysis

The error for each bending modulus data point was determined via error propagation using an error of 20% in k_{eff} , 10% for the tube outer diameter D , half the lateral pixel width in the force map for the tube length L and lengths on each side of the loading position (a , b), and the standard error in the linear fit for the effective spring constant of the tube k_{eff} .

Investigation of Inner and Outer Tube Diameter

Because one of the limitations of AFM three-point bending experiment is that the inner tube diameter cannot be determined, we have examined our TEM data in further detail in order to better estimate the upper bound of the increase in bending modulus that a hollow tube would give rise to. The inner and outer tube diameters of 24 nanotubes from the same batch of nanotubes used for the AFM measurements are shown in the table below:

Table 1: Tube Diameter Measurements

Tube #	D_{outer} (nm)	D_{inner} (nm)	D_i/D_o
1	64.179	28.358	0.441858
2	33.772	12.665	0.375015
3	22.586	9.079	0.401975
4	64.801	27.763	0.428435
5	20.301	11.367	0.559923
6	27.883	12.308	0.441416
7	45.394	24.841	0.547231
8	45.663	18.158	0.397652
9	27.261	12.006	0.440409
10	30.782	13.089	0.425216
11	35.87	15.256	0.425314
12	47.479	21.657	0.456139
13	67.531	21.739	0.321911
14	27.353	10.184	0.372317
15	35.515	17.519	0.493285
16	47.974	24.234	0.505149
17	67.758	27.888	0.411582
18	32.101	17.622	0.548955
19	56.399	18.293	0.32435
20	46.32	16.362	0.353238
21	35.639	9.289	0.260641
22	28.914	8.979	0.310542
23	31.452	14.917	0.474278
24	17.932	6.044	0.337051

The smallest and largest D_i/D_o ratios are highlighted in red. A smaller ratio corresponds to a more “solid” tube, i.e. thick tube wall, whereas a larger ratio corresponds to a thin-walled tube. The ratio of D_i/D_o ranges from 0.26 to 0.56 for this set of 24 tubes. Using the ratio of 0.56 as the upper bound, the bending moduli calculated in this study are potentially underestimated by ~10%.

Force Mapping Technique

For further description of the force mapping technique and how it can be used for mechanical property mapping, please see the following references:

Sullan, R.M.A. et al. Cholesterol-dependent nanomechanical stability of phase-segregated multicomponent lipid bilayers. *Biophysical Journal* **99** (2010) 507-516.

Ip, S.; Li, J.K.; Walker, G.C. Phase segregation of untethered zwitterionic model lipid bilayers observed on mercaptoundecanoic-acid modified gold by AFM imaging and force mapping. *Langmuir* **26** (2010) 11060-11070.